Contents lists available at Mapta Publishing Group

Vol. 1, No. 3, December, 2018

Mapta Journal of Architecture, Urbanism and Civil Engineering (MJAUCE)

journal homepage: http://maptapublishing.com/index.php/mjauce

ISSN: 2631-3243

Investigation on Corrosion Effects of Reinforcement on the Moment-Curvature Diagram of Reinforced Concrete Sections

Daniel Sobhani[a], Sajad Zarei[b], Hamid Reza Savoj[b], Mohsen Ali Shayanfar[c,*]

[a] *Rehabilitation and Retrofitting Research Centre, Iran University of Science and Technology, Tehran, Iran*
[b] *School of Civil Engineering, Iran University of Science and Technology, Tehran, Iran*
[c] *The Centre of Excellence for Fundamental Studies in Structural Engineering, Iran University of Science and Technology, Tehran, Iran*

Article Info

Article history:

Received Aug 28th, 2018
Revised Oct 9th, 2018
Accepted Nov 5th, 2018

Keyword:

RC structures
Reinforcement corrosion
Moment-curvature curve
Structural safety

Abstract

Corrosion of reinforcements in RC structures by changing the properties of concrete and steel, causing various damages in these structures, which ignoring it can lead to early destruction of the structure, in addition to causing various damages. In present research, considering the types of corrosion mechanisms of reinforcement in concrete, the negative effects of corrosion on mechanical properties and cross-section of reinforcement, as well as on cracking and strength reduction of concrete have been studied. Then moment-curvature analysis of section is performed to provide plastic hinges in nonlinear analysis of concrete frames exposed to corrosion. For this purpose, the beam sections with different percentages of reinforcement are analyzed in non-corrosion and under different corrosion rates. The major results of this research and of similar analyzes are namely the reduction in final moment and the change in final curvature of RC sections due to the severe corrosion of reinforcement.

1. Introduction

Nowadays, many RC structures are affected by various surface or internal failures, which corrosion of reinforcement is one of the causes of these failures, which needs to be studied and inspected. Corrosion of reinforcement occurs usually under special environmental conditions or when the poor construction materials are used for concrete or inadequate monitoring on concrete performance [1, 2]. Studies on structures constructed in coastal and warm areas indicate that corrosion of reinforcement is one of the most damaging factors in concrete structures that has harmful effects on the strength, stiffness, ductility and deformation capacity of members in these structures [3]. By assessing the effects of these damages on behavior of RC sections, the nonlinear behavior models of members of these structures need to be improved to better reflect the effects of corrosion on the reinforcement. Non-linear static analysis of major members of a RC-frame is interpretable using moment-curvature relationships. The curvature value of a concrete section depends on the cross-sectional specifications and the strain created therein. Therefore, by placing the strain of cross-section against the moment increase until the point of failure, the moment-curvature curve is obtained, so that the bending behavior in the plastic hinge region to be expressed as a relation between the applied bending moment and the curvature [4]. The use of moment-curvature curve in order to examine the effect of corrosion of reinforcement on behavior of concrete structures' members goes back to about 25 years ago, where Ting and Novak employed for RC beams [5]. In recent years, due to the importance of reinforcement corrosion in concrete structures, this case has been considered by various researchers. Ghanooni-Bagha et al. studied the effects of crack on chloride ingress and corrosion initiation of concrete samples by studying the finite element method [6]. Shayanfar et al. provided a developed model that considers the effects parameters on corrosion initiation in reinforcement [7] based on a developed model for reliability analisys by Kaveh et al. [8]. Ou et al. conducted a research on corrosion effect upon seismic performance in 9 concrete beam samples [9]. Kivell and colleagues performed a numerical study on effects of corrosion and corrosion-induced enclosure reductions of stirrup on the bonding failure and moment-curvature curve by means of a multiple spring model. And finally, the

* Corresponding author: shayanfar@iust.ac.ir

seismic performance of structure under corrosion is investigated by performing 60 trials of one-direction and cyclic drag tests [10]. The effect of cavity corrosion on reducing the cross-sectional reinforcement and also reducing the length of plastic hinge is considered in this study. Moment-curvature analysis of different cavity corrosion scenarios showed a decrease in ultimate moment of section (due to the reduction in cross-section of reinforcement) and the absence of a change in ultimate curvature of section [11]. Comparison of moment-curvature diagrams for different corrosion values indicated that with increasing corrosion, the cross-sectional moment capacity and energy absorption decreases and curvature is higher for lower moment values [12]. The FEMA-356 instruction for retrofitting the structures exposed to corrosion suggests the use of moment-curvature diagram of undamaged sections with anKnowledge Factor of 0.75 [13]. Since this coefficient is independent of the percentage of corrosion and resulted damage rate, thus in current study, to obtain an accurate moment-curvature curve by considering the corrosion effects under different degrees of corrosion is suggested, as an appropriate and more precise alternative for the Knowledge Factor.

2. Effects of reinforcement corrosion on steel and concrete properties

2.1. Change in mechanical properties of steel and the cross-section of reinforcement

One of the corrosion effects of reinforcement in concrete structures is the reduction of steel yield and ultimate stress by increasing corrosion [14]. In addition, the ductility and deformation of steel is reduced by increasing corrosion and the behavior becomes brittle [15]. Laboratory results of Rodriguez et al. showed a reduction of 30% and 50% in maximum strain for 15% and 28% reduction of RF cross-section caused by corrosion [16] Lee and Cho presented a model for defining the relationship between corrosion rate of reinforcement and the mechanical properties (in particular the yield strength and modulus of elasticity) of steel through several tests on various laboratory samples. The model by Lee and Cho is provided for evaluating and calculating the decrease rate in yield strength and the modulus of elasticity of steel based on the corrosion rate of reinforcement in both types of corrosion (uniform and pitting or cavity corrosion), where (1) and (2) relations are as following for uniform and pitting corrosion [17].

$$\sigma_{cy} = \left(1 - 1.24\frac{\Delta_w}{100}\right)\sigma_{sy} \qquad E_{cs} = \left(1 - 0.75\frac{\Delta_w}{100}\right)E_{ss} \tag{1}$$

$$\sigma_{cy} = \left(1 - 1.98\frac{\Delta_w}{100}\right)\sigma_{sy} \qquad E_{cs} = \left(1 - 1.15\frac{\Delta_w}{100}\right)E_{ss} \tag{2}$$

Where in these relations, σ_{cy} and$E_{cs}$are respectively the yield strength and the elasticity modulus of damaged reinforcement, where σsy and Ess are respectively the yield strength and elasticity modulus of reinforcement without corrosion, and Δw is rate of corrosion.

Another corrosion effect of reinforcement in RC structures is the reduction of reinforcement cross-section [18]. Depending on the type of corrosion created in the RC structures, various relationships are presented to calculate the residual diameter of reinforcement after corrosion. Rodriguez et al. presented relation (3) for uniform type of corrosion. This model calculates the amount of reduction in diameter of the reinforcement, based on the time elapsed since the beginning of corrosion process and the corrosion rate of reinforcement.

$$\varphi_t = \varphi_0 - \alpha P_x \tag{3}$$

φ0 is the initial diameter of armature and φt is the residual diameter of armature after t years since starting of corrosion, and α is the coefficient determined by the type of corrosion. For distributed corrosion (uniform), the value of α is 2. Further, Px is the mean value of depth of corrosion penetration in millimeters, which is calculated from equation (4) [19].

$$P_x = 0.0116 i_{corr}(t - t_{in}) = 0.0116 i_{corr}(t_p) \tag{4}$$

In this equation, $t_{in}$is the time it takes to start the corrosion in terms of years, and $t_p$is the corrosion expansion time in terms of year. And $i_{corr}$is the average corrosion rate or corrosion density in μA/cm2. To calculate the average corrosion rate, Vu et al. [20] provided the relationships.

In the case of pitting corrosion, according to the model provided by Val and Melchers [21], the maximum corrosion penetration into the armature is between four and eight times the average corrosion intrusion in the uniform type. In mentioned model, the radius of the hemisphere resulting from the corrosion penetration is calculated by equation (5).

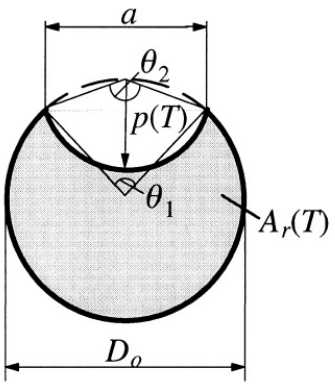

Figure 1. Pitting corrosion of reinforcement in Val & Melchers model [21]

$$P(T) = 0.0116\, i_{corr}\,(t - t_{in})R \tag{5}$$

Where R is the ratio between the maximum and the average corrosion penetration into the armature, where Val and Melchers proposed a numerical value of 4 to 8 for that. The residual area of reinforcement surface after the impact of pitting corrosion can be calculated from relations (6) to (8), according to Figure1.

$$A_r(T) = \frac{\Pi D_0^2}{4} - A_1 - A_2 \qquad P(T) \le \frac{\sqrt{2}}{2} D_0 \tag{6}$$

$$A_r(T) = A_1 - A_2 \qquad \frac{\sqrt{2}}{2} D_0 < P(T) \le D_0 \tag{7}$$

$$A_r(T) = 0 \qquad P(T) > D_0 \tag{8}$$

2.2. Reduction of concrete compressive strength

Another corrosion effect is applied on the RC materials' specification, concrete cracking and loss of concrete coating. Due to the increased volume caused by the chemicals processed during the corrosion process (iron oxidation), radial compressive force is created along the reinforcement surfaces and causes the tensile stresses in the concrete surround the reinforcement. In the low and medium corrosion, cracking and then the layering occurs; and in the severe corrosion, the spilling occurs in entire coating of concrete. To considering the reduction in compressive strength of concrete, some researchers proposed relationships, e.g.GhanooniBagha and Shayanfar [22, 23].

2.3. Reduction in structural ductility and change in failure mechanism

As the corrosion rate increases, the structural ductility decreases due to the reduction of cross-sectional area and the loss of continuity. Conducted studies shows that 60% corrosion resulted the behavior same as the unreinforced concrete [24]. In addition to decrement in strength and ductility of the structure, the corrosion of reinforcement can cause large changes in the mechanism of failure. For example, under the certain conditions that the columns of a story level are more exposed to corrosion than other members of the structure, then the ductile failure mode (in which the plastic hinges are formed at the two ends of the beam) can turn into a brittle failure mode (formation of plastic hinges in columns and leading to create the soft floor).

3. Modeling the behavior of materials

3.1. Strain-strain model of concrete at pressure

For the modeling of concrete in the compression area, the Kent and Park models modified by Scott [25] have been used in accordance with relations (9) to (11), which are respectively related to the ascending region, descending region and the residual stress of concrete.

$$\sigma_c = Kf'_c \left[2\left(\frac{\varepsilon_c}{\varepsilon_{c0}}\right) - \left(\frac{\varepsilon_c}{\varepsilon_{c0}}\right)^2 \right] \qquad \varepsilon_c \le \varepsilon_{c0} \tag{9}$$

$$\sigma_c = Kf'_c\left[1 - Z\left(\varepsilon_c - \varepsilon_{c0}\right)\right] \qquad \varepsilon_{c0} \le \varepsilon_c \le \varepsilon_u \tag{10}$$

$$\sigma_c = 0.2Kf'_c \qquad \varepsilon_c \ge \varepsilon_u \tag{11}$$

In the above relations, ε_{c0}= 0.002K, which is the concrete strain corresponding to maximum stress, and K is the strength coefficient increasing due to the enclosure, and Z is the slope of the descending branch of the stress-strain curve at the pressure, calculated from the following relationships:

$$K = 1 + \frac{\rho_s f_{yh}}{f'_c} \tag{12}$$

$$Z = \frac{0.5}{\frac{3 + 0.0284 f'_c}{14.21 f'_c - 1000} + 0.75\rho_s\sqrt{\frac{h'}{s_h}} - 0.002K} \tag{13}$$

Where f_{yh} and f'_c, the yield stress of stirrups and compression strength of concrete, are in *kg/cm*^{2}. And ρ_s is the volume ratio of the stirrup reinforcement to the concrete core enclosed by bars (up to the outer layer of stirrups); further, *h'* and $S_h$are respectively the width of enclosed concrete core and the distance between the stirrups from each other.

3.2. Stress-Strain Model of Steel

The model used to describe the stress-strain relationship of steel consists of two regions. The first region is the linear elastic and the second region is linear re-hardening. In general, the assumption of the re-hardening behavior immediately after the yielding of steel reinforcement is correct if the gradient of re-hardening region is determined in such a way that the strain energy of the model is equal to the strain energy of the stress-strain relationship of the steel obtained from the test. In other words, the area below the bilinear diagram and the real stress-strain curve should be the same. Typically, a slope of 0.03 is a proper value [4].

4. Nonlinear analysis with moment-curvature curve

4.1. An Introduction to moment-curvature curve

Since a structure consists of a large number of structural members and a member consists of the aggregation of sections, it can be said that nonlinear behavior of a cross section causes nonlinear behavior in the structure. In the case of beams and columns, which are the main constituent parts of a frame, internal forces are usually concentrated in sections that are located at both ends and middle of the member. Due to this feature of the structure, plastic hinge analysis is widely used in nonlinear analysis and structural retrofitting. The bending behavior in the plastic hinge region is expressed as a relation between the applied bending moment and the curvature (the strain slope created along the cross section) [26].

The moment-curvature relation for a cross-section is determined using cross-section analysis method, so that the conditions of strain compatibility, force equilibrium and stress-strain relations are satisfied. This method is based on the Bernoulli theory that the plain sections remain flat after bending, as well as stress-strain relations are defined for steel and concrete. The analysis involves determining the depth of the neutral axis for a certain curvature value using the axial equilibrium and then using the rotational equilibrium to calculate the bending moment corresponding to the curvature.

4.2. Moment-Curvature trilinear model

A moment-curvature relationship for a reinforced concrete cross section can be idealized as a trilinear relationship. This relation consists of three regions: 1) the elastic region before cracking 2) the formation and expansion of the cracks 3) the steel yielding zone till the failure. For a better understanding, the ductile member behavior is shown in Figure 2.

The slope of Moment-Curvature curve denotes elastic flexural strength (EI), which includes cross-sectional properties under specified loading conditions. According to the figure, the effect of cracking and yielding of steel is well obvious on reducing the stiffness and creating the nonlinear behavior.

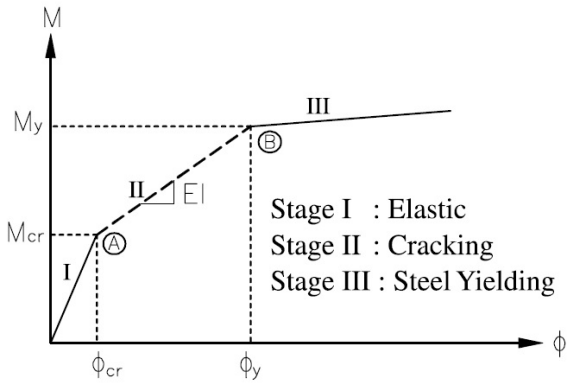

Figure 2- Moment-Curvature trilinear diagram [2]

5. Case study and interpretation of analytical results

In the following research, three models are considered as the case study to investigate the effect of corrosion on moment-curvature behavior of cross-section. In the first model, a beam of reference [4] has been selected, and a moment-curvature curve has been extracted numerically for non-corrosion and uniform corrosion with low and high intensity, regarding the effect of corrosion on compressive strength of concrete and the ultimate strain of steel. In the second model, a concrete cross section with different percentages of reinforcement has been investigated, and the effect of the loss of cover has also been studied. For this purpose, the corrosion of pitting type and its effect on compressive strength of concrete and yield strength and elasticity modulus of steel are considered.

5.1. Numerical example of obtaining the moment-curvature curve for a beam

Based on the discussion in section 2, the moment-curvature curve calculations for a two-headed beam are performed, according to its cross-sectional characteristics presented in details in Table (1).

Table 1. Cross-sectional specifications of T1MA beam

f_y (kg/cm²)	f_c (kg/cm²)	E_s (kg/cm²)	E_c (kg/cm²)	ρ’	ρ	d (cm)	H (cm)	B (cm)
3236	323	1980000	271000	0	0.0062	27.23	15.24	30.45

Determination of point A, corresponding the first crack: at the crack point A, in accordance with Figure 1, the strain at the last tensile bar of concrete is equal to cracking strain of concrete. At this point, the concrete has elastic behavior in tensile and compression (Figure 3). Then:

$$\varphi_{cr} = \frac{\varepsilon_{cr}}{H - c} \tag{14}$$

$$c = \frac{BH \times \frac{H}{2} + (n-1)A_s d + (n-1)A'_s\, d'}{BH + (n-1)A_s + (n-1)A'_s} \tag{15}$$

$$\Rightarrow c = 15.63cm, \varphi_{cr} = 9.4\times10^{-6}, M_{cr} = 9.79\times10^{4}\, kg.cm$$

$$M_{cr} = \frac{1}{3}\varepsilon_{cc}E_c c^2 B + \frac{(c-d')^2}{c}\varepsilon_{cc}E_s A_{sc} + \frac{1}{3}\frac{(H-c)^3}{c}\varepsilon_{cc}E_c B + \frac{(d-c)^2}{c}\varepsilon_{cc}E_s A_{st} \tag{16}$$

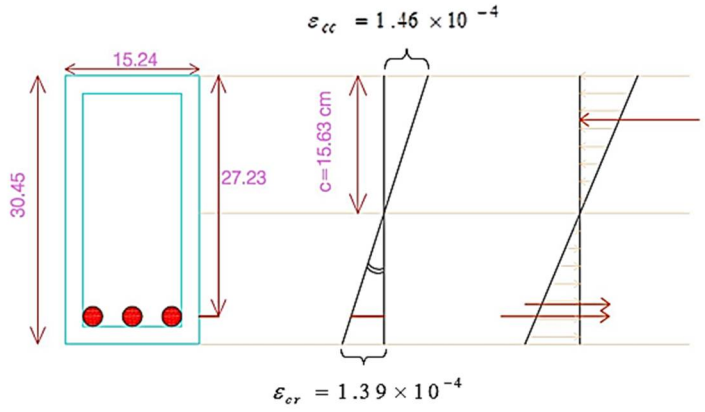

Figure 3. Strain-stress diagrams corresponding to the cracking at the first tensile bar

Determination of point B, corresponding to yielding (Figure 4): at yielding point of B assuming that the strain in tensile reinforcements reaches the steel's yield strain, the neutral point is estimated, and by trial and error, the neutral bar is determined so that force equilibrium is maintained at section, that is, the difference between tensile and compressive forces is to be less than a certain value.

$$T = \sigma_{st} A_s + \int_{A_{tc}} \sigma_{tc} dA = f_y A_s + \int_{A_{tc}} \sigma_c dA \tag{17}$$

$$C = \sigma_{sc} A'_s + \int_{A_{cc}} \sigma_c dA \tag{18}$$

$$\Rightarrow c = 9.05cm, \quad \varphi_y = \frac{\varepsilon_y}{d-c} = 8.07 \times 10^{-5}, M_y = 2.14 \times 10^5 kg.c$$

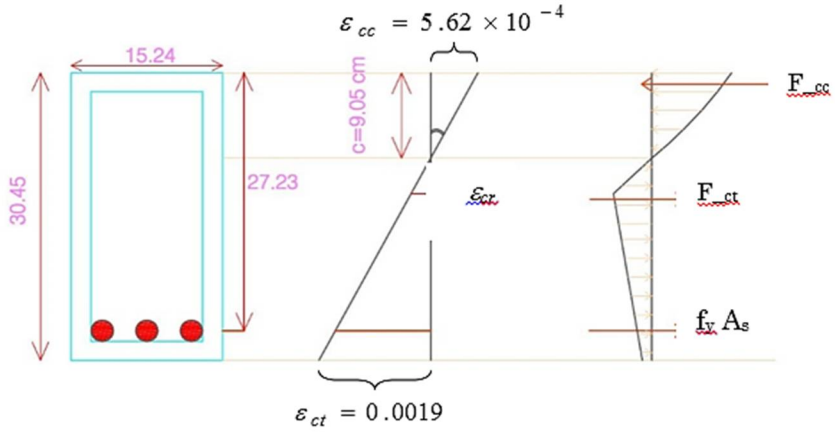

Figure 4. Strain-stress diagram corresponding to the yielding

Determination of ultimate point (Figure 5): After the yielding of tensile reinforcement, the moment-curvature curve continues to be a straight line with a slope of $E_{s2} I_{cr}$, which E_{s2} is the modulus of elasticity of steel after the yielding, while the bending capacity of section depends entirely on the behavior of steel at this stage [4]. Thus, without regard to the reference (2)'s proposal, to obtain the ultimate point and in accordance with the suggestion of chapter 9 of Iranian National Building Regulations (INBR), the strain at the last compression bar equals with 0.0035, and by trial and error the neutral bar's height is found so that the forces applied to the cross section are equal to zero:

$$C = \text{F\_cc} = 1.25 \times 10^4 kg$$

$$T = \mathrm{F\_ct} + F_s = 676 + 1.17 \times 10^4 = 1.25 \times 10^4 kg$$

$$\Rightarrow c = 3.43cm, \quad \varphi_u = \frac{\varepsilon_{cc}}{c} = 0.001, M_u = 3.28 \times 10^5 kg.cm$$

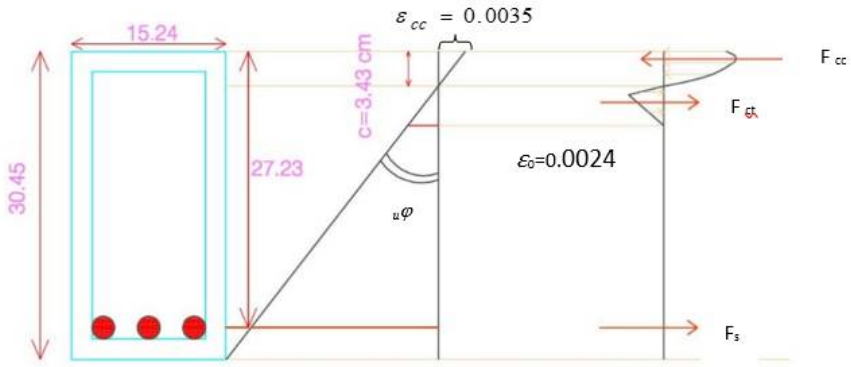

Figure 5. Strain-stress diagram corresponding to the ultimate point

Subsequently, according to the reference [3], two uniform corrosions are considered to be 6% and 25%, respectively, as low and high intensity corrosion rate.

The summing up of the above results as well as the results of cross-sectional analysis in MATLAB software under the corrosion rates of 6% and 25% are as follows:

Table 2 - Analysis results of the beam section

	0%		6%		25%	
	Curvature	Moment	Curvature	Moment	Curvature	Moment
0	0	0	0	0	0	0
Cracking Point	0.0000094	97900	0.00000859	89100	0	0
Yielding point	0.000807	214000	0.00008197	197600	0.000079	161600
Ultimate Point	0.001	306000	0.0009676	278000	0.00073	220300

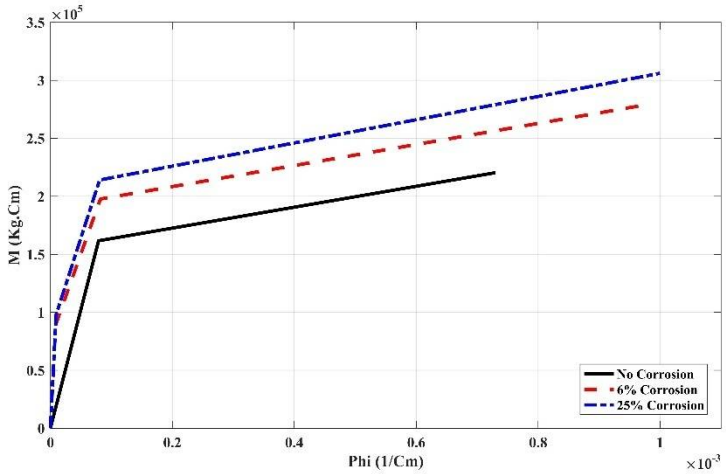

Figure 6. Moment-Curvature curve of T1M1 beam at various rate of corrosion

It can be seen that the positive moment in the corrosion of 6% and compared to the non-corrosion state, the ultimate moment and curvature have decreased by 8% and 4%, respectively. In the corrosion of 25%, the ultimate moment has been reduced by 30%, where the ultimate curvature has increased by 36%, which is due to the crusting and removal of concrete cover from the section, thus reduces the stiffness of cross section and causes more curvature in lower moment.

The reduction of curvature in low-corrosion percentages and its increment is consistent with the graphs given in reference [12]. It should be noted that in high intensity corrosion, the section is severely cracked and the cracking correspondent point appears at the beginning and before loading.

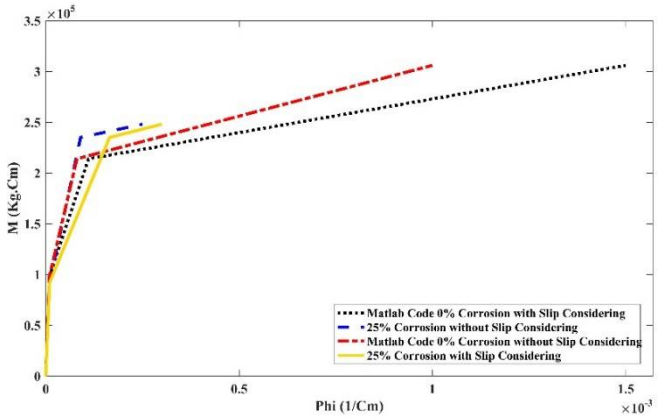

Figure 7. Moment-Curvature curve of T1M1 beam regarding the slip effect

The Moment-Curvature behavior of beam has been investigated in corrosion-free and the corrosion modes of low and high intensity.

5.2. Beam cross-sections with different reinforcement percentage

The modelled sections are the support sections of a beam from an RC frame with dimensions of 50 to 70 cm. The strength of concrete is 350 Kg / cm2, the yield strength of reinforcement is 4200 Kg / cm2, and the concrete density is 2300 Kg / m3. The steel elastic modulus is 2,000,000 Kg / cm2, and the modulus of elasticity of concrete is obtained from the following equation:

$$E_C = 33 \cdot \left(W_C^{1.5} \cdot \sqrt{f_C{}'} \right) \tag{19}$$

In this regard, W_C is the specific weight of concrete ($\frac{lb}{ft^3}$), and $f_C{}'$ is the compressive strength of concrete (psi) (27).Other specifications of section are as follows:

$$E_C = 33 \cdot \left(W_C^{1.5} \cdot \sqrt{f_C{}'} \right) \tag{20}$$

Table 3. Section specifications of studied beam

Section	A_s (cm^2)		A_s' (cm^2)		ρ	ρ'	S (cm)
A	4φ22	15.2	4φ28	24.62	0.0043	0.007	10
B	6φ22	22.8	6φ28	36.93	0.0065	0.011	1611

In this study, the corrosion of bars is assumed to be of carbonate type, which caused the corrosion to be uniform. Also, the effect of reduced compressive strength of concrete is considered in accordance with Section 2-2, and the reduction of yield stress and elasticity modulus of steel is obtained from relation (1).Since the diameter of compressive and tensile bars are constant at both sections, then considering the start time of corrosion (T_{in}) does not affect the study.The moment-curvature behavior of beams for different corrosion rates (5% to 30%) is plotted using the MATLAB code, the results of which are presented in Figure 8.

5.2.1. Effect of changes in percentage of cross-section bars

In Figure 8, the moment-curvature curve of two sections mentioned above is observed for corrosion-free and corrosive conditions of 5% to 30%. As can be seen from the relations of reduced strength of concrete, the reduction in yield stress and the steel's modulus of elasticity, it can be concluded that the change in percentage of cross-sectional bars does not affect any of the above parameters. With the analysis done by the MATLAB code and the study of the above curves, it is observed that the reduction amounts of moment and curvature are equal with each other in both sections (the difference is at most 3%). As a result, it can be seen that changes in percentage of cross-sectional bars have no effect on moment and curvature variations (or have little change).

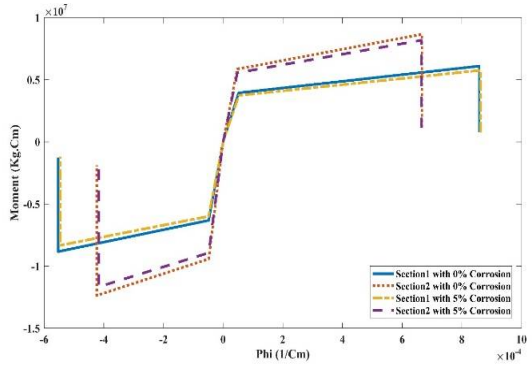

A) 10% corrosion and non-corrosion curves

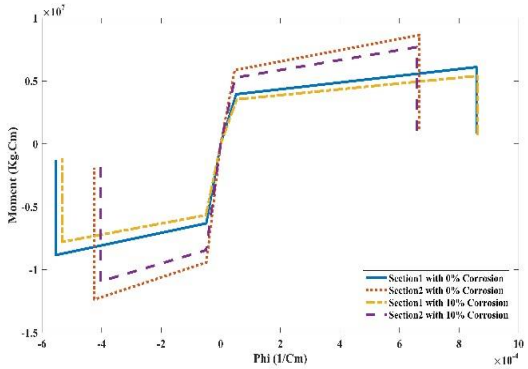

B) 10% corrosion and non-corrosion curves

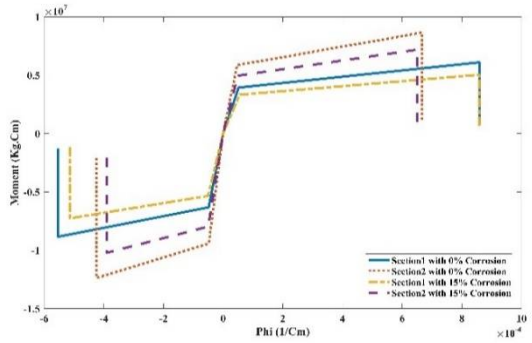

C) 15% corrosion and non-corrosion curves

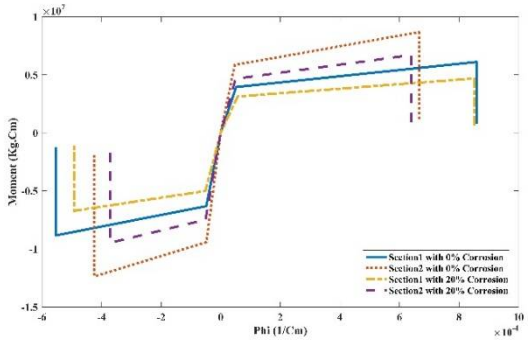

D) 20% corrosion and non-corrosion curves;

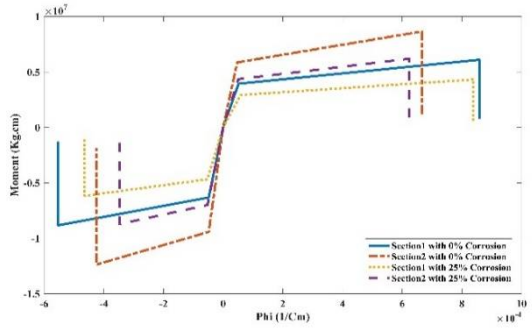

E) 25% corrosion and non-corrosion curves

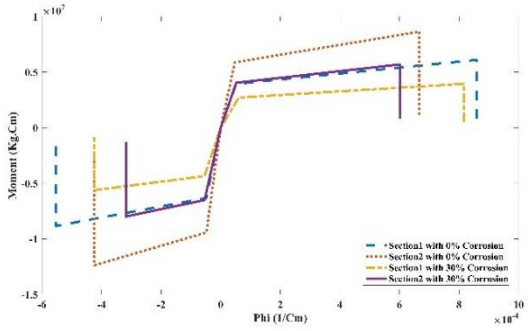

F) 30% corrosion and non-corrosion curves

Figure 8. Moment-curvature curves for different percentages of rebar in sections A and B

5.2.2. The effect of cover removal of cross-section on the moment-curvature curve

The beam section cover also has a significant effect on the moment-curvature behavior. When the cross-sectional bars are corroded, the loss of concrete cover increases the curvature and reduces the moment of the section, but if the

concrete cover is not damaged, then both the moment and curvature parameters are reduced. Thus, result of cover removal will have a significant effect on curvature variation. If the distance between corroded bars is less than the concrete cover value, then it can be concluded that the concrete cover will be removed before the cracks reach the concrete surface, as the cracks reach each other in a transverse direction (in the direction of bars).

The below figure represents moment-curvature curve of studied section in a non-corrosive state, and with a corrosion of 30% with coating, and a corrosion of 30% without the concrete coating. From the following curves it's concluded that removal of cover in the section with corroded bars increases the curvature up to 75%, when compared to the non-corrosive state, while in the section with corroded bars and cover, the value of curvature is reduced up to 20%.

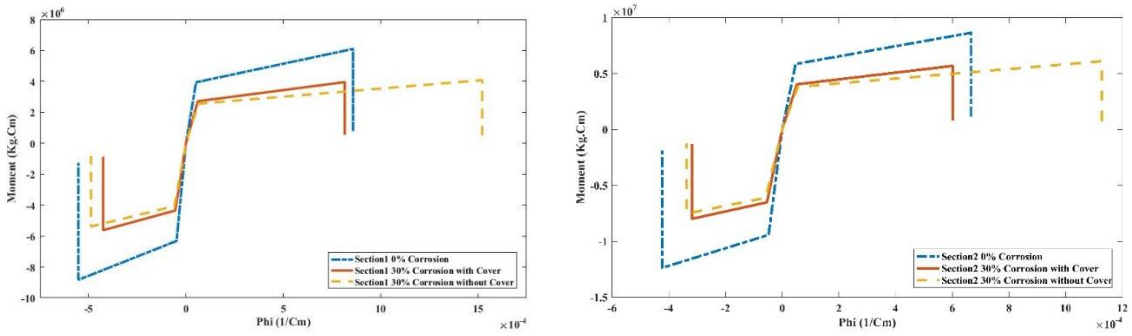

A) Section A **B) Section B**

Figure 9 - Without Corrosion, 30% Corrosion and 30% Corrosion with Spalling

6. Conclusions

In present research, first the effects of corrosion on the parameters of a concrete cross section is discussed, and then the moment-curvature curve is calculated for a concrete cross section. Finally, the corrosion effect for a cross section with various percentages of steel and also the effect of coating on the moment-curvature curve is discussed. Based on the analysis, the following results are obtained:

- In a low-intensity uniform corrosion, the ultimate moment and curvature of the section are slightly reduced compared to the non-corrosion state. However, in pitting corrosion considering all corrosion effects, even in low intensity corrosion, the ultimate curvature of section is slightly increased compared to the non-corrosion state.
- In extreme corrosion, the ultimate moment of section is significantly reduced, and the ultimate curvature is significantly increased. Though, in pitting corrosion without considering the corrosion effect on the yield strength and the steel modulus of elasticity, in severe corrosion also the ultimate curvature decreases.
- Sometimes in high intensity corrosion, the increase in ultimate curvature is small due to the change in failure mechanism and the achievement of reinforcement strain to the decreased ultimate strain (εsu) before the concrete reaches the ultimate strain.
- The FEMA 356 proposal on application of Knowledge Factor in capacity and the ductility (as deformation)for corrosion on force members is different from the results of Inci et al. (No change in the ultimate curvature caused by corrosion), Yalciner et al., and the diagrams of the present study. It is suggested that in FEMA 356 the Knowledge Factor for corrosion effects always to reduce the capacity, instead of deformation limit.
- The application of knowledge factor of 0.75 in sections capacity for low intensity corrosion, is non-economical, and for high intensity corrosion is unsafe.
- The result of FEMA 356 in non-corrosive state is slightly conservative.
- The reduction in concrete strength, yield stress and elasticity modulus of steel is equal for the sections with the same corrosion percentage, and the different percentage of reinforcement does not affect the mentioned parameters. (Assuming that the size of the bars and cover on bars are equal in sections, as this assumption leads to equalization of corrosion's starting time and the corrosion rate of bars)
- Changes in percentage of section's reinforcement will not affect the reduction of moment and curvature.

- The removal of coating after corrosion will reduce the value of moment, and increase the curvature, but if after the corrosion, the concrete cover of section is not damaged, then both the moment and curvaturedecrease.

Acknowledgment

Authors are grateful to Mohammad Ghanooni-Bagha, Department of civil Engineering, East Tehran Branch, Islamic Azad University for his assistance in all of aspect for perform this research.

References

[1] M.A. Shayanfar, M.A. Barkhordari, M. Ghanooni-Bagha. Estimation of corrosion occurrence in RC structure using reliability based PSO optimization. Periodica Polytechnica Civil Engineering. 59 (2015) 531-42.

[2] M. Ghanooni Bagha. Influence of effective chloride corrosion parameters variations on corrosion initiation. Modares Civil Engineering journal. 17 (2017) 69-77.

[3] P. Simioni. Seismic response of reinforced concrete structures affected by reinforcement corrosion. thèse de Doctorat du: Faculty of Architecture, Civil Engineering and …2009.

[4] H.-G. Kwak, S.-P. Kim. Nonlinear analysis of RC beams based on moment–curvature relation. Computers & structures. 80 (2002) 615-28.

[5] S.-C. Ting, A.S. Nowak. Effect of reinforcing steel area loss on flexural behavior of reinforced concrete beams. Structural Journal. 88 (1991) 309-14.

[6] M. Ghanooni-bagha, M. Shayanfar, M. Farnia. Cracking effects on chloride diffusion and corrosion initiation in RC structures via finite element simulation. Scientia Iranica. (2018).

[7] M.-A. Shayanfar, M.-A. Barkhordari, M. Ghanooni-Bagha. Probability calculation of rebars corrosion in reinforced concrete using css algorithms. Journal of Central South University. 22 (2015) 3141-50.

[8] A. Kaveh, M. Massoudi, M.G. Bagha. Structural reliability analysis using charged system search algorithm. Iranian Journal of Science and Technology Transactions of Civil Engineering. 38 (2014) 439.

[9] Y.C. Ou, L.L. Tsai, H.H. Chen. Cyclic performance of large‐scale corroded reinforced concrete beams. Earthquake Engineering & Structural Dynamics. 41 (2012) 593-604.

[10] A. Kivell, A. Palermo, A. Scott. Corrosion related bond deterioration and seismic resistance of reinforced concrete structures. Structures Congress 20122012. pp. 1894-905.

[11] P. Inci, C. Goksu, A. Ilki, N. Kumbasar. Effects of reinforcement corrosion on the performance of RC frame buildings subjected to seismic actions. Journal of Performance of Constructed Facilities. 27 (2012) 683-96.

[12] H. Nazarnia, H. Sarmasti. Characterizing Infrastructure Resilience in Disasters Using Dynamic Network Analysis of Consumers' Service Disruption Patterns. Civil Engineering Journal. 4 (2018) 2356-72.

[13] F. Prestandard. commentary for the seismic rehabilitation of buildings (FEMA356). Washington, DC: Federal Emergency Management Agency. 7 (2000).

[14] C.A. Apostolopoulos, V. Papadakis. Consequences of steel corrosion on the ductility properties of reinforcement bar. Construction and Building Materials. 22 (2008) 2316-24.

[15] A. Mostafavi, N.E. Ganapati, H. Nazarnia, N. Pradhananga, R. Khanal. Adaptive capacity under chronic stressors: Assessment of water infrastructure resilience in 2015 Nepalese earthquake using a system approach. Natural Hazards Review. 19 (2017) 05017006.

[16] J. Rodriguez, C. Andrade. CONTECVET A validated users manual for assessing the residual service life of concrete structures. Geocısa, Madrid, Spain. (2001).

[17] H.-S. Lee, Y.-S. Cho. Evaluation of the mechanical properties of steel reinforcement embedded in concrete specimen as a function of the degree of reinforcement corrosion. International journal of fracture. 157 (2009) 81-8.

[18] M.A. Shayanfar, M.A. Barkhordari, M. Ghanooni-Bagha. Effect of longitudinal rebar corrosion on the compressive strength reduction of concrete in reinforced concrete structure. Advances in Structural Engineering. 19 (2016) 897-907.

[19] J. Rodriguez, L. Ortega, J. Casal. Corrosion of reinforcing bars and service life of reinforced concrete structures: corrosion and bond deterioration. International conference on concrete across borders, Odense, Denmark1994. pp. 315-26.

[20] K.A.T. Vu, M.G. Stewart. Structural reliability of concrete bridges including improved chloride-induced corrosion models. Structural safety. 22 (2000) 313-33.

[21] D.V. Val, M.G. Stewart, R.E. Melchers. Effect of reinforcement corrosion on reliability of highway bridges. Engineering structures. 20 (1998) 1010-9.

[22] M. Ghanooni-Bagha, M. Shayanfar, A. Shirzadi-Javid, H. Ziaadiny. Corrosion-induced reduction in compressive strength of self-compacting concretes containing mineral admixtures. Construction and Building Materials. 113 (2016) 221-8.

[23] M. GhAnooni-BAGhA, M.A. ShAyAnfAr, O. Reza-Zadeh, M. Zabihi-Samani. The effect of materials on the reliability of reinforced concrete beams in normal and intense corrosions. Eksploatacja i Niezawodność. 19 (2017).

[24] H. Nazarnia, A. Mostafavi, N.E. Ganapati, N. Pradhananga, R. Khanal. Assessment of infrastructure resilience in developing Countries: A case study of water infrastructure in the 2015 Nepalese earthquake. (2016).

[25] B. Scott, R. Park, M. Priestley. Stress-strain behavior of concrete confined by overlapping hoops at low and high strain ratio Rates. Doctoral Thesis, Lulea University of Technology, Lulea, Sweden1989.

[26] M. Shayanfar, H. Savoj, M. Ghanoonibagha, A. Khodam. The effects of corrosion on seismic performance of reinforced concrete moment frames. Journal of Structural and Construction Engineering. 5 (2017) 146-59.